Physiol Genomics 41: 254–268, 2010.
First published March 9, 2010; doi:10.1152/physiolgenomics.00006.2010.

Gene expression in hypothalamus, liver, and adipose tissues and food intake response to melanocortin-4 receptor agonist in pigs expressing melanocortin-4 receptor mutations

C. Richard Barb,[1] Gary J. Hausman,[1] Romdhane Rekaya,[2] Clay A. Lents,[2] Sender Lkhagvadorj,[3,4] L. Qu,[3,5,6] W. Cai,[3,5] Oliver P. Couture,[3,6] Lloyd L. Anderson,[3,4] Jack C. M. Dekkers,[3,6] and Christopher K. Tuggle[3,4,6]

[1]*Poultry Processing and Swine Physiology Research, Agricultural Research Service, United States Department of Agriculture;* [2]*Department of Animal and Dairy Science, University of Georgia, Athens, Georgia;* [3]*Department of Animal Science,* [4]*Interdepartmental Neuroscience Program,* [5]*Department of Statistics, and* [6]*Interdepartmental Bioinformatics and Computational Biology Program, Iowa State University, Ames, Iowa*

Submitted 11 January 2010; accepted in final form 2 March 2010

Barb CR, Hausman GJ, Rekaya R, Lents CA, Lkhagvadorj S, Qu L, Cai W, Couture OP, Anderson LL, Dekkers JC, Tuggle CK. Gene expression in hypothalamus, liver, and adipose tissues and food intake response to melanocortin-4 receptor agonist in pigs expressing melanocortin-4 receptor mutations. *Physiol Genomics* 41: 254–268, 2010. First published March 9, 2010; doi:10.1152/physiolgenomics.00006.2010.— Transcriptional profiling was used to identify genes and pathways that responded to intracerebroventricular injection of melanocortin-4 receptor (MC4R) agonist [Nle^4, D-Phe^7]-α-melanocyte stimulating hormone (NDP-MSH) in pigs homozygous for the missense mutation in the MC4R, D298 allele ($n = 12$), N298 allele ($n = 12$), or heterozygous ($n = 12$). Food intake (FI) was measured at 12 and 24 h after treatment. All pigs were killed at 24 h after treatment, and hypothalamus, liver, and back-fat tissue was collected. NDP-MSH suppressed ($P < 0.004$) FI at 12 and 24 h in all animals after treatment. In response to NDP-MSH, 278 genes in hypothalamus ($q \leq 0.07$, $P \leq 0.001$), 249 genes in liver ($q \leq 0.07$, $P \leq 0.001$), and 5,066 genes in fat ($q \leq 0.07$, $P \leq 0.015$) were differentially expressed. Pathway analysis of NDP-MSH-induced differentially expressed genes indicated that genes involved in cell communication, nucleotide metabolism, and signal transduction were prominently downregulated in the hypothalamus. In both liver and adipose tissue, energy-intensive biosynthetic and catabolic processes were downregulated in response to NDP-MSH. This included genes encoding for biosynthetic pathways such as steroid and lipid biosynthesis, fatty acid synthesis, and amino acid synthesis. Genes involved in direct energy-generating processes, such as oxidative phosphorylation, electron transport, and ATP synthesis, were upregulated, whereas TCA-associated genes were prominently downregulated in NDP-MSH-treated pigs. Our data also indicate a metabolic switch toward energy conservation since genes involved in energy-intensive biosynthetic and catabolic processes were downregulated in NDP-MSH-treated pigs.

melanocyte-stimulating hormone; microarray; hypothalamus; MC4R

THE CURRENT KNOWLEDGE OF FACTORS regulating voluntary food intake in humans and domestic animals is very limited. The majority of this knowledge is based on studies in rodents (52, 70). Numerous reports have demonstrated that the hypothalamic melanocortin system plays a major role in regulating appetite and energy homeostasis (1, 8, 14). The regulation of the melanocortin system is via the melanocortin receptor agonist, alpha-melanocyte stimulating hormone (α-MSH), which is derived from proopiomelanocortin (POMC), and the antagonist, agouti-related protein (AgRP). Both AgRP and POMC have been identified in the hypothalamus of the pig (19, 44), and their action is mediated by the melanocortin-3 and 4-receptor (MC3R and MC4R; 22, 23). In mice, central administration of AgRP or the MC4R antagonist SHU9119 robustly increased feeding behavior, indicating that antagonism of the MC4R is an important orexigenic signal (27, 73). In POMC and MC4R knockout mice (9) and mice overexpressing AgRP (29), the same obese phenotype is exhibited. A similar phenotype was observed in humans with mutations in MC4R (24). Thus, a functional MC4R plays a pivotal role in the regulation of energy homeostasis.

Rothschild and coworkers identified a missense mutation (D298N) in the porcine MC4R (pMC4R) gene that changes a highly conserved aspartic acid in TM7 in melanocortin receptors to asparagine (42). Moreover, this missense mutation is associated with increased food intake, growth, and fatness (42). A structure and function relationship has been observed in natural and experimentally induced MC4R mutations in humans (69, 51) and mice (53). Furthermore, highly conserved residues in the MC4R protein structure may be critical for ligand binding and signal transduction (59, 68). Recent findings revealed that cell lines transfected with the porcine MC4R D298N mutation had decreased cAMP production when stimulated with the MC4R agonist compared with cells transfected with the wild-type receptor (43). In direct contrast to this report, Fan et al. (23), using the same experimental paradigm, demonstrated that in cells transfected with MC4R, the D298N mutation failed to alter MC4R signaling or cAMP content. We have previously reported that central administration of a MC3/4R agonist,[Nle^4, D-Phe^7] (NDP)-MSH, suppressed food intake in pigs. In contrast treatment with a MC3/4R antagonist, SHU9119, failed to stimulate intake, whereas AgRP ability to increase feeding behavior was equivocal (6). Moreover, these pigs were heterozygous for the MC4R mutation. Clearly, further work is needed to understand the functional role of MC4R on the genetic and metabolic pathways involved in appetite and growth. Therefore, the purpose of the present study was, first, to test the idea that food intake response to intracerebroventricular (ICV) injection of the MC4R agonist, NDP-MSH, is MC4R genotype dependent and, second, to determine whether genes and pathways that respond to central

Address for reprint requests and other correspondence: C. R. Barb, USDA, ARS, Richard B. Russell Agriculture Research Center, 950 College Station Rd., Athens, GA, 30605 (e-mail: Richard.barb@ars.usda.gov).

administration of NDP-MSH are affected in pigs with alternate MC4R genotypes.

MATERIALS AND METHODS

Twelve crossbred prepuberal gilts and six male castrates, 64 ± 2 kg body weight, and 130–140 days of age were used. Pigs were screened for MC4R genotype with a missense mutation in the MC4R (D298N; 42), which has been associated with increased food efficiency. Pigs homozygous for MC4R, D298 allele ($n = 6$), or N298 allele ($n = 6$) or heterozygous ($n = 6$) were selected from the University of Georgia swine herd (PIC composite). In a complete 2 × 3 factorial design, within each genotype, two gilts and one male were assigned to each of the hormonal treatments. All pigs were surgically implanted with lateral ICV cannulas with the stereotaxic procedure of Estienne et al. (20) and Barb et al. (5). Animals were individually penned in an environmentally controlled building at a constant temperature of 22°C and artificial 12:12-h light-dark photoperiod. Pigs were fed ad libitum a corn-soybean meal ration (14% crude protein) supplemented with vitamins and minerals, according to the National Research Council (NRC) guidelines (57). One week after the last ICV surgery, feeders were removed at 0700, ICV injections of 150 μl 0.9% saline ($n = 9$) or 10 μg of the MC3/4R agonist [Nle^4, D-Phe^7]-α-MSH (NDP-MSH; Bachem, Torrance, CA; $n = 9$) were administered at 0800, feeders were placed in all pens, and food intake was monitored at 12 and 24 h after feed presentation. All pigs were killed 24 h postinjection, and hypothalamus, liver, and 10th rib middle layer of subcutaneous adipose tissue were collected as previously described (4, 33). mRNA was isolated as described previously (30, 32) and was hybridized to Affymetrix Gene Chip Porcine Genome Arrays containing 24,123 probe sets. A second replicate was conducted as described above with an additional 12 prepuberal gilts and six castrate males averaging 77 ± 2 kg and 140 days of age; within each genotype, two gilts and one male were assigned to each of the treatments. This resulted in the following groups for the two replicates: saline ($n = 6$/D298, $n = 6$/N298, $n = 6$/D298N), 10 μg NDP-MSH ($n = 6$/D298, $n = 6$/N298, $n = 6$/D298N). All procedures were approved by the Richard B. Russell Agriculture Research Center Committee on Animal Care and Use.

Isolation of Total RNA

Total RNA was isolated from hypothalamus, liver, and adipose tissues for each pig ($n = 36$ pigs) by extraction with QIAzol Lysis Reagent (Qiagen, Valencia, CA) followed by isopropanol precipitation of the aqueous phase. RNA was resuspended in water and immediately purified on Qiagen's RNEasy Mini Columns according to the manufacturer's procedure. Total RNA quality and quantity were determined by microfluidic analysis on an Agilent 2100 Bioanalyzer (Agilent Technologies, Foster City, CA). Each RNA extract was divided into aliquots for use with Affymetrix Gene Chips, and for quantitative real-time PCR (qPCR) on liver and adipose from each of the 36 animals and hypothalamus from 32 of the 36 were used. Four of the hypothalamus samples had been used up for the microarrays. Theses included two heterozygous females (one control and one treated) and two N298 animals (one female control and one male treated).

Affymetrix Arrays

Affymetrix GeneChip Porcine Genome Arrays (Affymetrix, Santa Clara, CA) were processed at Yerkes Microarray Core at Emory University in Atlanta, GA. Standard labeling of target (one round amplification), hybridization to GeneChip Porcine Genome Arrays (hybridization, washing, staining, and scanning), and data extraction and analysis were carried out on an Affymetrix GeneChip Instrument System (GeneChip Scanner 3000, Fluidic Stations 450, Hybridization Oven 640, and computer workstation loaded with GeneChip Operating Software) using the manufacturer's reagents and protocols. Target was prepared using Affymetrix's One-Cycle Eukaryotic Target Labeling Assay with 5 μg total RNA as starting material. Briefly, the RNA was reverse-transcribed into double-stranded complementary deoxyribonucleic acid (cDNA), which was subsequently transcribed into biotin-labeled complementary RNA with simultaneous amplification. The resulting target was hybridized to GeneChip Porcine Genome Arrays.

Gene Ontology Biological Process Enrichment and Pathway Analysis

Annotation of human homologs of the Affymetrix porcine probe sets (67) with gene names and Gene Ontology (GO) enrichment analysis was performed by tools available at DAVID Bioinformatics Resources (18). The transcriptome background for each tissue consisted of all genes flagged as present, marginal, or unknown on at least one of the GeneChip Porcine Genome Arrays for that tissue and that were matched to a human homolog. Redundancies caused by multiple probe sets that were annotated to the same gene were eliminated. This resulted in a transcriptome of 10,866 genes for hypothalamus, 10,484 genes for liver, and 10,681 genes for adipose tissue. For GO enrichment analysis, the lists of differentially expressed genes ($q \leq 0.07$) were divided into up and down expression by tissue, and redundant genes were eliminated. Each list was analyzed for overrepresentation (enrichment $P \leq 0.1$) in all levels of GO Biological Processes using DAVID's Gene Functional Annotation tool with medium stringency settings. GO enrichment cluster themes were denoted by the biological process with the smallest P value for each cluster. For pathway analysis, the top 50 most differentially expressed (up or down) genes by fold change in adipose tissue and genes with log fold changes of ≥ 0.57 and ≤ −0.57 in hypothalamus and liver were analyzed for overrepresentation in KEGG pathways (Kyoto Encyclopedia of Genes and Genomes, release 49.0) (38–40). Pathway themes were determined by KEGG orthology identifiers in KEGG's BRITE database.

qPCR

Custom Taqman Gene Expression Assays (forward primer, reverse primer, and 6FAM dye: MGB-labeled probe) were designed by Applied Biosystems (Foster City, CA) from sequences that were based on GenBank or The Institute for Genomic Research (TIGR) Pig Gene Index records and that were assessed for quality according to Applied Biosystems guidelines (Table 1). A custom porcine 18S rRNA assay was designed as an endogenous control. We transcribed 3 μg total RNA was transcribed into cDNA in a volume of 20 μl with Superscript III First-Strand Synthesis System (Invitrogen, Carlsbad, CA) utilizing random hexamers and following the manufacturer's protocol (25°C for 10 min, 50°C for 50 min). The cDNA was diluted 1:10 for use as template in the amplification reaction. The amplification reaction consisted of 1 μl diluted cDNA, 10 μl iQ Supermix (Bio-Rad Laboratories, Hercules, CA), 0.8 μl 20× custom TaqMan Gene Expression Assay, and water up to a total volume of 20 μl. To measure each assay's probe reaction efficiency, a series of 20 μl reactions was performed similar to the above using as template 1 μl of a threefold to 2,187-fold range of serial dilutions of a pool of all available cDNAs. PCR was performed in Bio-Rad's CFX 96 Real-Time PCR Detection System. Thermal cycling parameters were as follows: an initial denaturation step (95°C for 10 min), followed by 40 cycles of denaturation and annealing/extension (95°C for 15 s, 60°C for 1 min) in a 96-well optical plate.

Analysis of qPCR data

C_t (threshold cycle) values were determined using Bio-Rad's CFX Manager Software. Automatic background fluorescence and thresholds were checked, and no adjustments were determined necessary. Within-sample triplicate well reactions that did not fall within one

Table 1. *Primer pair, probe sequence, and GenBank accession number for each gene*

Gene	Symbol	GenBank Accession Number	1. Forward Primer Sequence (5′ to 3′) 2. Reverse Primer Sequence (5′ to 3′) 3. Reporter Sequence (5′ to 3′)	Design Strand	Amplicon Length, bp
3-beta-Hydroxysteroid dehydrogenase/delta-5-delta-4 isomerase	*3B-HSD*	NM_001004049	1. GCGCCGTACCCCTTGA 2. AGAGCCCAGCCGTTAGC 3. TCAGCCAGCTTTTTGC	reverse	65
Acyl-CoA synthetase long-chain family member 3	*ACSL3*	NM_001143698	1. TGAGTCAAGGCAAGAAAAATCAAACC 2. AGCCAAACCATCCAAGCTGTTAA 3. ACAGGCTTTGCTTTAATG	reverse	100
ADP-ribosylation factor-like protein 3	*ARL3*	NM_001031785	1. GTAATTGACAGCGCAGACAGAAAA 2. GCACTGGAACACAACTTAGCTTTT 3. ACGGGTCAGGAACTAG	forward	94
Angiogenin	*ANG1*	NM_001044573	1. ACCTTTATTCATGGCACGAGGAA 2. AGGAGACTTGCTTCTTCTGAAATTGT 3. AAGGCCATCTGTAATGAT	forward	93
Angiopoietin-like 4	*ANGPTL4*	NM_001038644	1. ACTGCCAAGAGCTGTTTGAAGA 2. CCATCTGAGGTCATCTTGCAGTTAA 3. CTTTGCCGCTCTCCC	reverse	106
Cytochrome c oxidase subunit VIIc	*COX7C*	NM_001097474	1. CAGGGAAGAATTTGCCATTTTCAGT 2. CAGCAAATCCAGATCCAAAGTACAG 3. CCGCCACTTATTTTC	reverse	84
Epidermal growth factor receptor	*EGFR*	NM_214007	1. TGATCCAGGCTGTCTCAATGG 2. GCTGGGCACAGATGACTTTG 3. ACTGCCAGAAATTGAC	forward	83
Fatty acid binding protein 3, muscle and heart (mammary-derived growth inhibitor)	*FABP3*	NM_001099931	1. TTCGGGAACTAGTTGATGGGAAAC 2. CGTAAGTGCGAGTGCAAACTG 3. TCATCCTGACACTCACCC	forward	72
Fatty acid synthase	*FASN*	NM_001099930	1. GCTTGTCCTGGGAAGAGTGTAAG 2. CACCGTGTCTTTGGAGTTGTG 3. CAGCGCTGCCCCC	forward	77
Galactosylceramidase	*GALC*	CF793186	1. GGCTTCCTGCCATGACAGAATTA 2. GTTGACCGTGTGTCTGAGTGA 3. CCCACGACGAGGACAC	forward	63
Interleukin 15	*IL15*	NM_214390	1. TTTAACTGAGGATGGCATTCATGTCTT 2. GCCAGGTTGCTTCTGTTTTAGGA 3. CTGATACAGCCCAAAATG	reverse	77
Karyopherin alpha 4	*KPNA4*	AY010067	1. GCTCAGCCACCAGGAAGTT 2. TGCCCACAGCTCGAAGTG 3. CTGCTGTCTGAACTTT	reverse	53
Leptin	*LEP*	NM_213840	1. GACGATTGTCACCAGGATCAGT 2. CGGTGACCCTCTGTTTGGA 3. CACATGCAGTCTGTCTCC	forward	68
Lipoprotein lipase	*LPL*	NM_214286	1. TGGCATTGCAGGAAGTCTGA 2. GGCTTGGAGCTTCTGCATACTC 3. ATCTAGGCCAGTAATTCT	reverse	95
Malate dehydrogenase 1, NAD (soluble)	*MDH1*	NM_213874	1. GCTGCCTTGGACAAATATGCTAAGA 2. CAGTTGGTATTGGCTGGGTTTC 3. CCACCACGATAACCTT	reverse	71
NAD(P)H dehydrogenase, quinone 1	*NQO1*	BQ601005	1. AGATTCTGTCTTTTCTTTCTCCAAGCA 2. CACCCAACTCCTCAATGGTCTTA 3. CTCTTCTGCCATAAACCA	forward	94
Neuropeptide Y	*NPY*	AF264083	1. TCGGCGTTGAGACATTACATCA 2. GTCTCGGGACTAGATCGTTTTCC 3. CACCAGGCAGAGATAC	forward	68
Symplekin	*SYMPK*	CN158843	1. GGCCTGTTGCTCTGTATATTCTGT 2. ACTTTACAGTTCTTTTCCCAGATGCT 3. ATGCCATGCTATGTCTAACA	forward	79
Solute carrier family 1 (neuronal/epithelial high-affinity glutamate transporter, system Xag), member 1	*SLC1A1*	AY195622	1. TCTCCTGACAGCTCTCATGATCTC 2. AGCACAGCGGAAAGTGACA 3. CTCCAGTTCAGCAACACT	forward	64
Uncoupling protein 3	*UCP3*	NM_214049	1. ACCATCGCCAGGGAGGAA 2. CCTCGTGATGTTGGGCAGAATT 3. CCTTTCCACAGGCCCC	reverse	63
Phosphodiesterase 4D[1]	*PDE4D*	EF109889	AAGTTCTGGAGTTCTTCTTCTTGAT[3]	N/A	119
Protein kinase, cGMP-dependent, type I[2]	*PRKG1*	NM_001044574	TCATTCTGATTTCATAGTGAGATTA[3]	N/A	117

[1]Noncustom Taqman Gene Expression Assay ID Ss03377183_u1; target exon 9. [2]Noncustom Taqman Gene Expression Assay ID Ss03388356_g1; target exon 1. [3]Context sequence of noncustom Taqman Gene Expression Assay.

cycle of each other were repeated, and the original reactions were excluded from analysis. The C_t values of within-sample triplicate wells were averaged. Relative differences in gene expression were calculated by the Relative Expression Software Tool (REST) procedure (60). Sample, endogenous control, and probe reaction efficiency C_ts were imported into REST V2.0.7 2008 (Corbett Research, Sydney, Australia). Biological replicates were not averaged before import. Statistical significance was set at ($P \leq 0.05$), and the reference gene was 18S rRNA. The ratio compared the expression of treated to untreated. Ratios are reported as -1 divided by the ratio if downregulated to correct for nonlinear appearance, with positive numbers indicating upregulation, negative numbers indicating downregulation, and a ratio of 1 indicating no differential expression.

Analysis of Affymetrix Data

Data preprocessing. The background adjustment was done in R using the Affymetrix Bioconductor software, which is a widely used program for the analysis and interpretation of data arising from high-throughput experimentation in genomics and molecular biology. Probe intensities were adjusted based upon a weighted average of the backgrounds for each region. The weights are based on the distances between the location of the probe and the centroids of 16 different regions. Although perfect match (PM) and mismatch (MM) probe level can be used in the statistical analysis, several studies (13) have reported the limited contribution of MM data as well as the potential for adding more noise; consequently, only PM data were used in this study.

A scaling/linear method for normalizing the raw Affymetrix data was used in the analysis. This method was implemented by selecting a baseline array and then fitting a linear regression without intercept term between each array and the chosen array. The resulting fitted regression line is used as the normalizing relationship. We used the Affymetrix package of the Bioconductor for preprocessing the raw data; it has many methods for background adjustments as well as data normalization of Affymetrix microarray data. The log base 2 transformation was performed on the background-adjusted and normalized PM intensities as suggested by previous studies (37).

Statistical analysis. In typical microarray experiments, several systematic and random effects contribute to the observed variation in the data. The use of mixed linear models for the analysis of microarray data (74) provides a flexible tool for accommodating these effects.

In this study, the following mixed linear model was used to analyze the probe level intensities for every gene separately: $PM_{ijklmo} = \mu + tr_i + geno_j + array_k + sex_l + (tr*geno)_{ij} + e_{ijklmo}$, where PM_{ijklmo} is the $\log_2$-transformed intensity for probe for gene m for sample o, trt_i is the treatment effect ($i = 1,2$); $geno_j$ is the effect of genotype ($j = 1,2,3$), $array_k$ is the random effect of array ($k = 1,2,...36$), sex_l is the effect of sex ($l = 1,2$), $(trt*geno)_{ij}$ is the interaction effect between treatment and genotype, and e_{ijklmo} is the residual term. It is important to note that the number of probes per gene ranged from 11 to 20. Furthermore, the following assumptions were made about the distribution of the random effects in the model: $e_{ijk} \sim N(0, \sigma_e^2)$ and $A_k \sim N(0, \sigma_a^2)$, where σ_e^2 and σ_a^2 are the within and between array variances, respectively. Proc mixed of Statistical Analysis System (SAS; 48) was used for fitting the mixed linear model, and the restricted maximum-likelihood method was used to estimate the variance components.

The contrast statement was used to estimate and test linear combinations of interest. Degrees of freedom for F-test were estimated using the satterthwaite option in SAS proc mixed. Least-square estimates of both treatments for each single gene were calculated using the LSMEANS statement of SAS.

Multiple comparisons. Due to the large number of genes tested in microarray studies a method to assess the number of false positives is of great importance. In this study, the Hochberg-Benjamini method (36) for false discovery rate calculation was used to account for the multiple comparisons. The method can be summarized in the following three steps:

1) For a given significance level, α_e, genes were ranked by their P values from the most to the least significance.

2) A threshold value was calculated for each gene as: $Threshold_i = (R_i*\alpha_e)/N$, where R_i is the rank of gene i and N is the total number of genes in the array.

3) Each P value was then compared with its respective threshold, starting with the most significant P value, until a P value greater than the threshold value is encountered.

Statistical Analysis of Feed Intake Data

To determine the effect of treatment and genotype on feed intake across time, data were subjected to the general linear model split plot-in-time ANOVA procedure of SAS (63). The statistical model included treatment, pig, genotype, replicate, and time. Effects of treatment were tested using animal within dose as the error term. Time was tested using dose × time as the error term and dose × time was tested by the residual. Differences between treatment means within a time were determined by least-squares contrasts (63).

RESULTS

NDP-MSH suppressed ($P \leq 0.004$) food intake at 12 and 24 h in all animals after treatment (Fig. 1). There was no replicate, genotype, or treatment × genotype interaction detected ($P \geq 0.8$). Although NDP-MSH treatment suppressed food intake, these animals consumed enough feed to meet maintenance requirements according to NRC requirements for swine.

Microarray Data Validation

Expression of unique upregulated and several downregulated genes in the microarray analysis of NDP-MSH treatment and controls was verified by qPCR in fat, liver, and hypothalamic tissue (Table 2). In fat, these included downregulated lipid biosynthetic genes, i.e., fatty acid synthase (FASN) and lipoprotein lipase (LPL). Upregulated genes included 3-beta-hydroxysteroid dehydrogenase/delta-5-delta-4 isomerase (HSD3B1), angiopoietin-like-4 (ANGPTL4) and uncoupling protein 3 (UCP3). Other noteworthy genes not verified in-

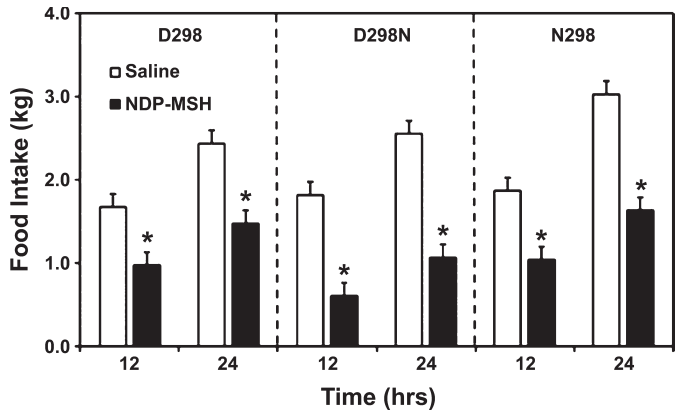

Fig. 1. Cumulative food intake (mean ± SE) for pigs homozygous for melanocortin-4 receptor (MC4R), D298 allele ($n = 12$), N298 allele ($n = 12$), or heterozygous ($n = 12$). Six pigs from each genotype received intracerebroventricular (ICV) injections of 150 μl saline or 10 μg of the MC3/4R agonist [Nle^4, D-Phe^7] melanocyte-stimulating hormone (NDP-MSH). There was no replicate or treatment × genotype interaction detected ($P > 0.8$). Times at which effects of treatment were different from saline-treated animals *($P < 0.004$).

Table 2. *Microarray data validation on a subset of differentially expressed genes ($q \leq 0.07$) by qPCR in liver, hypothalamus, and adipose tissue*

	Microarray		qPCR	
Gene Symbol	Log 2 Fold Change	*P* Value	Ratio	*P* Value
	[1]Liver			
ACSL3	−0.463	2.29E-04	−1.239	9.23E-02
FABP3	−0.614	3.51E-04	−1.260	9.20E-02
GALC	0.486	5.61E-04	1.520	7.00E-03
NQO1	−0.920	4.87E-04	−1.149	2.40E-03
MDH1	−0.275	2.61E-04	−1.270	2.00E-03
COX7C	−0.335	3.12E-04	−1.253	2.00E-02
ARL3	−0.357	3.92E-05	−1.280	1.00E-03
	[2]Hypothalamus			
GALC	−0.333	3.96E-06	1.290	3.21E-01
KPNA4	0.269	1.62E-06	1.350	7.00E-03
NPY	0.738	8.61E-03	2.326	1.31E-02
SLC1A1	0.172	6.30E-04	1.293	2.30E-02
PDE4D	−0.522	6.05E-05	1.339	1.06E-02
PRKG1	0.853	1.01E-07	1.242	6.02E-02
SYMPK	−0.517	1.16E-05	−1.626	1.98E-01
	[1]Adipose Tissue			
FASN	−1.162	2.06E-06	−2.513	0.001
LPL	−0.566	6.51E-07	−1.745	0.001
UCP3	0.595	3.47E-05	1.640	8.00E-03
3B-HSD	0.594	2.08E-05	2.523	9.00E-03
LEP	−0.817	2.29E-06	−2.421	2.40E-02
ANGPTL4	1.4128	3.88E-08	1.830	1.80E-02
ANG1	0.657	3.15E-07	1.275	8.90E-02
IL-15	0.491	3.72E-06	1.113	3.55E-01
EGFR	0.636	8.15E-06	1.233	1.00E-01

[1]$n = 36$; [2]$n = 32$. Official gene symbols: ACSL3, acyl-CoA synthetase long-chain family member 3; ANG1, angiopoietin-1; ANGPTL4, angiopoietin-like-4; ARL3, ADP-ribosylation factor-like 3; COX7C, cytochrome c oxidase subunit VIIc; EGFR, epidermal growth factor receptor; FABP3, fatty acid binding protein 3; FASN, fatty acid synthase; GALC, galactosylceramidase; 3B-HSD, hydroxy-delta-5-steroid dehydrogenase, 3 beta- and steroid delta-isomerase 1; IL-15, interleukin 15; KPNA4, karyopherin alpha 4; LEP, leptin; LPL, lipoprotein lipase; MDH1, malate dehydrogenase 1, NAD; NPY, neuropeptide Y; PDE4D, phosphodiesterase 4D, cAMP-specific; PRKG1, protein kinase, cGMP-dependent, type I; SYMPK, symplekin; NQO1, NAD(P)H dehydrogenase, quinone 1; SLC1A1, solute carrier family 1 member 1; UCP3, uncoupling protein 3.

cluded interleukin 15 (IL-15), and angiogenin (ANG1). In liver, downregulated genes included lipid biosynthetic and energy metabolism genes, i.e., NAD(P)H dehydrogenase, quinone 1; malate dehydrogenase-1, Nad (MDH1); and cytochrome C oxidase subunit 7c (COX7C). In the hypothalamus, statistical significance of the fold changes of solute carrier family 1 member 1, karyopherin-α4, and neuropeptide Y (NPY) was verified by qPCR ($P \leq 0.05$). Overall, the results obtained from microarray were confirmed for these sets of genes. For all the tested genes, fold changes in expression were consistent in direction compared with the microarray results except in adipose tissue for IL-15 ($P = 0.3$), epidermal growth factor receptor (EGFR, $P = 0.10$), and ANG1 ($P = 0.09$) despite substantial Log2 fold changes of 0.49 for IL-15, 0.64 for EGFR and 0.66 for ANG1, in liver for ACLS3 ($P = 0.09$) and FABP3 ($P = 0.09$) with Log2 fold changes of −0.46 and −0.60, respectively, and in hypothalamic tissue for phosphodiesterase 4D, cAMP-specific (PDE4D, $P = 0.01$), galactosylceramiase ($P = 0.3$), and symplekin (SYMP, $P = 0.2$) with Log2 fold changes of −0.52, −0.33, and −0.52, respectively. Overall, the results obtained from microarray were statistically confirmed for 70% of the tested genes in the hypothalamus, liver, and fat by qPCR.

MC4R Effects on Expression of Genes in Adipose Tissue, Liver, and Hypothalamus

A total of 5,066 transcripts were identified to be differentially expressed ($q \leq 0.07$, $P \leq 0.015$) in adipose tissue, with 3,276 being upregulated and 1,790 downregulated. In liver, 249 transcripts were identified to be differentially expressed ($q \leq 0.07$, $P \leq 0.001$), of which 163 were upregulated and 86 downregulated. In hypothalamic tissue, 278 transcripts were identified as differentially expressed ($q \leq 0.07$, $P \leq 0.001$), with 56 being upregulated and 222 downregulated. For simplicity, changes in RNA levels detected by these probe sets will be referred to as gene expression differences. The gene-by-gene analysis that was conducted identified evidence of effects of the MC4R genotype (290, 41, 1, transcripts identified, respectively) and an interaction between genotype × treatment (1,724, 40, 2 transcripts identified, respectively) at $q \leq 0.07$.

Interaction of Genotype × Treatment in Adipose Tissue, Liver, and Hypothalamus

Animals were used in each combination of experimental factors ($n = 6$/genotype/treatment); every effort was made to balance the design by assigning animals with similar weight and sex distribution to each group to avoiding potential confounding with genotype by treatment interaction. On the basis of stringent significance levels, several genes showed a clear genotype × treatment interaction in food intake at 12 and 24 h after MSH injection, for all three tissues considered in this study. In fact, 1,724, 40, and 2 genotype × treatment interactions were detected for adipose tissue, liver, and hypothalamus, respectively. To further investigate these interactions, especially for adipose tissue and liver, we profiled the expression of some genes with significant interaction using both the normalization PM data and the correspondent LSMEANS obtained during the statistical analysis. For all nine selected genes (5 for adipose tissue and 4 for liver) a clear interaction was observed using normalized PM and LSMEANS (Figs. 2 and 3 and Supplementary Figs. S4 and S5, Supplementary Tables S6 and S7).[1] These results suggest a real genetic control of gene expression sensitivity to MSH treatment that could indicate a difference in genetic background for these and for the three genotypes considered in this study. The large number of significant interactions between MSH treatment and MC4R genotype observed for adipose tissue demonstrates its dynamic and complex role in the regulation of food intake.

Biological Processes Affected by NDP-MSH Treatment in the Hypothalamus, Liver, and Adipose Tissue

To identify biological processes that respond to ICV administration of NDP-MSH, differentially expressed genes in hypothalamic, liver, and fat tissue were analyzed for overrepresentation in GO Biological Process categories and KEGG biological pathways (Supplementary Figs. S4 and S5, Supple-

[1] The online version of this article contains supplemental material.

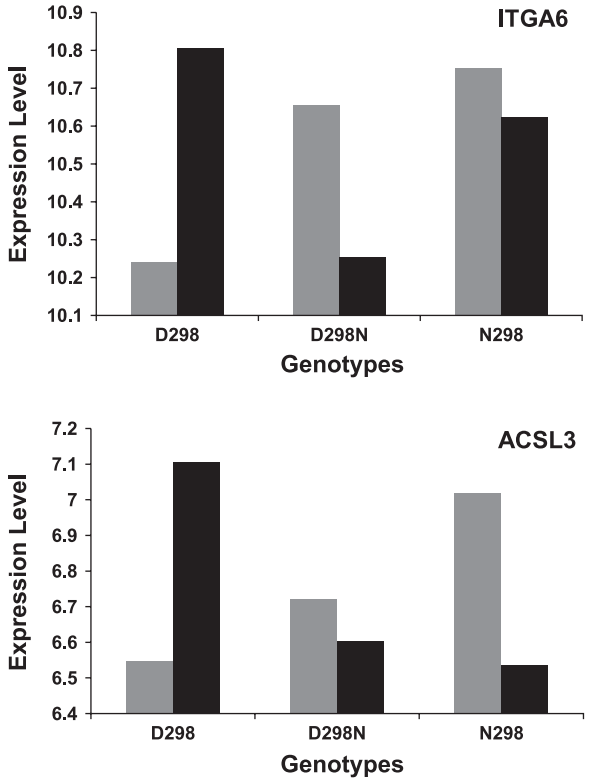

Fig. 2. Adipose tissue gene expression profiles for acyl-CoA synthetase long-chain family member 3 (ACSL3) and integrin alpha 6 (ITGA6) with a genotype × treatment interaction ($P \leq 0.0001$). Values in the *y*-axis are LSMEAN ($n = 6$/genotype/treatment). Black bars represent saline controls, and gray bars represent NDP-MSH treatment.

mentary Tables S6–S12). In addition, the KEGG biological pathway database was used to identify specific biological pathways overrepresented by genes that responded to NDP-MSH treatment in the hypothalamus, liver, and fat ($P \leq 0.05$, Tables 3–5). Results are described further in following sections.

NDP-MSH Effects on Hypothalamic and Liver Gene Expression

Hypothalamic tissue underwent significant downregulation of transcriptional changes in response to NDP-MSH. Major groups of genes associated with biopolymer metabolism, cyclic nucleotide metabolism, and protein amino acid phosphorylation were downregulated. In particular, genes involved in cell communication, nucleotide metabolism, signal transduction, amino acid metabolism, and lipid metabolism were predominantly downregulated (Table 3 and Supplementary Table S8).

The extent of significant downregulated transcriptional regulation changes in liver tissue was considerable and involved genes associated with lipid biosynthesis and glucose catabolism. The genes found to be differentially regulated in liver and overrepresented ($P \leq 0.05$) in KEGG pathways were identified (Table 4 and Supplementary Table S9). Of the 15 genes annotated by KEGG to encode for enzymes and binding proteins in lipid biosynthesis, the majority were downregulated, including the rate-limiting FABP1–3 involved in the peroxisome proliferator-activated receptor (PPAR) signaling pathway. In addition, genes involved in nucleotide metabolism, amino acid metabolism, and energy metabolism, such as carbonic anhydrase III (CA3) and COX7C, were downregulated (Table 4). Genes associated with gluconeogenesis, lactate dehydrogenase-C, glycan biosynthesis, and metabolism were upregulated (Table 4).

In liver tissue the effect of genotype in the response to MSH was not as robust as observed in adipose tissue; GO enrichment cluster analysis for genotype did not detect any cluster themes.

Effects of MSH Treatment on Adipose Tissue

The scope of the significant downregulated transcriptional regulation changes in adipose tissue was considerable and surprising and involved major groups of genes associated with both anabolic and catabolic processes. In particular, genes involved in direct energy-generating processes such as oxidative phosphorylation, electron transport, ATP synthesis, and the citric acid cycle (TCA) were prominently downregulated in NDP-MSH-treated pigs (Table 5 and Supplementary Table S10). Our data also indicate a metabolic switch toward energy conservation since genes involved in energy-intensive biosynthetic and catabolic processes were downregulated in MSH-treated pigs. This included genes encoding biosynthetic pathways such as steroid and lipid biosynthesis, fatty acid synthesis, protein translation, amino acid synthesis, and ubiquinone biosynthesis, as well as genes encoding enzymes involved in catabolic processes such as proteolysis, amino acid degradation, and pyruvate metabolism. In particular, downregulation of genes

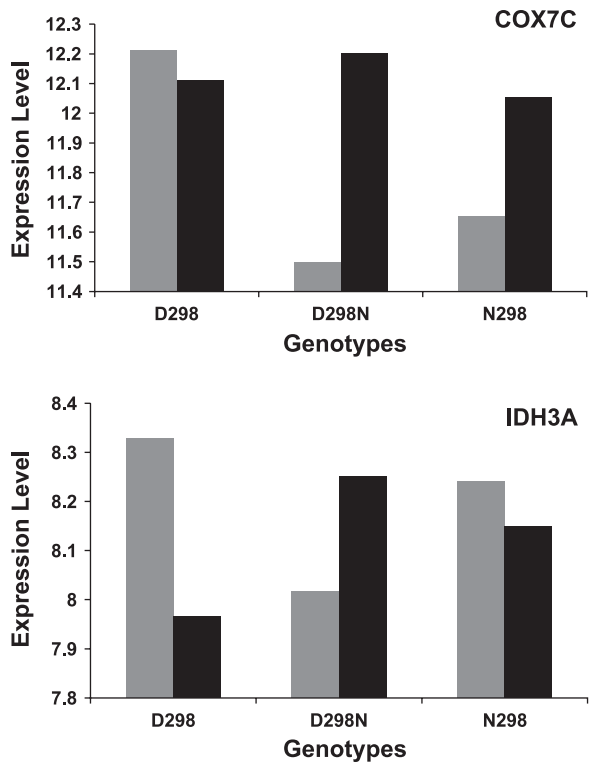

Fig. 3. Liver tissue gene expression profiles for cytochrome c oxidase subunit VIIc (COX7C) and isocitrate dehydrogenase 3 alpha (IDH3A) that exhibited a genotype × treatment interaction ($P \leq 0.0001$). Values in the *y*-axis are LSMEAN ($n = 6$/genotype/treatment). Black bars represent saline controls, and gray bars represent NDP-MSH treatment.

Table 3. *Hypothalamus tissue genes with false discovery rate correction (q-value) cutoff 0.07*

KEGG Pathway Theme/Gene Name*	Gene Symbol	Porcine Affy ID	Log2 Fold Change	*P* Value	q-value
		Amino Acid Metabolism			
Glutamate-cysteine ligase, modifier subunit	*GCLM*	Ssc.24693.2.S1_at	0.328	5.69E-05	2.45E-02
Branched chain aminotransferase 1, cytosolic	*BCAT1*	Ssc.27431.1.A1_at	0.295	2.60E-05	1.74E-02
Tyrosyl-tRNA synthetase	*YARS*	Ssc.16687.1.S1_at	0.142	4.36E-04	5.46E-02
Myst histone acetyltransferase (monocytic leukemia) 4	*MYST4*	Ssc.30919.1.A1_at	−0.189	2.74E-04	4.56E-02
Methylcrotonoyl-coenzyme A Carboxylase 2 (beta)	*MCCC2*	Ssc.27572.1.S1_at	−0.209	5.74E-05	2.43E-02
Procollagen-lysine, 2-oxoglutarate 5-dioxygenase 2	*PLOD2*	Ssc.24126.1.A1_at	−0.232	6.45E-04	6.30E-02
Serine hydroxymethyltransferase 1 (soluble)	*SHMT1*	Ssc.23145.1.A1_at	−0.322	5.71E-04	6.12E-02
Kiaa0828 protein	*KIAA0828*	Ssc.12833.1.A1_at	−0.411	1.11E-04	2.97E-02
		Carbohydrate Metabolism			
Tissue-specific transplantation antigen P35B	*TSTA3*	Ssc.18627.1.S1_a_at	0.172	4.02E-04	5.25E-02
Swi/Snf-related, matrix-associated, actin-dependent regulator of chromatin, subfamily A, member 2	*SMARCA2*	Ssc.1339.1.A1_at	−0.160	7.62E-04	6.81E-02
Inositol polyphosphate multikinase	*IPMK*	Ssc.18803.1.S1_at	−0.205	3.55E-04	5.01E-02
Chitobiase, Di-N-acetyl-	*CTBS*	Ssc.13500.1.A1_at	−0.243	9.09E-05	2.89E-02
		Cell Communication			
Protein kinase, cGMP-dependent, type I	*PRKG1*	Ssc.10791.1.A1_at	0.853	1.01E-07	1.22E-03
Protein kinase C, Iota	*PRKCI*	Ssc.7253.1.A1_at	0.304	2.17E-04	4.21E-02
Membrane-associated guanylate kinase, Ww And Pdz domain containing 2	*MAGI2*	Ssc.17432.1.S1_at	−0.165	4.40E-04	5.44E-02
Laminin, alpha 2 (merosin, congenital muscular dystrophy)	*LAMA2*	Ssc.12029.1.S1_at	−0.179	7.99E-04	6.96E-02
Myosin, heavy polypeptide 4, skeletal muscle	*MYH4*	Ssc.30625.1.S1_at	−0.204	9.50E-05	2.86E-02
Protein kinase C, epsilon	*PRKCE*	Ssc.8482.1.A1_at	−0.232	6.98E-04	6.47E-02
Caveolin 1, caveolae protein, 22 kDa	*CAV1*	Ssc.24958.1.A1_at	−0.242	2.08E-04	4.17E-02
Integrin, alpha 6	*ITGA6*	Ssc.14294.1.A1_at	−0.279	1.44E-04	3.48E-02
Keratin 10 (epidermolytic hyperkeratosis; keratosis palmaris et plantaris)	*KRT10*	Ssc.9782.1.A1_at	−0.299	8.27E-07	3.32E-03
Symplekin	*SYMPK*	Ssc.26722.1.S1_at	−0.517	1.16E-05	1.22E-02
		Cell Growth and Death			
Cell division cycle 27	*CDC27*	Ssc.27075.1.A1_at	−0.299	5.56E-04	6.04E-02
Cyclin H	*CCNH*	Ssc.26385.1.S1_at	−0.158	1.16E-04	3.02E-02
Cytochrome C, somatic	*CYCS*	Ssc.17412.1.A1_at	−0.159	7.04E-04	6.51E-02
		Development			
Unc-5 homolog C (*C. elegans*)	*UNC5C*	Ssc.10672.1.A1_at	−0.179	2.87E-04	4.49E-02
Actin-binding Lim protein 1	*ABLIM1*	Ssc.9560.2.S1_a_at	−0.193	2.54E-04	4.42E-02
		Ssc.10988.1.S1_at	−0.262	5.82E-04	6.11E-02
		Ssc.19823.1.A1_at	−0.267	6.34E-05	2.43E-02
		Endocrine System			
Exocyst complex component 7	*EXOC7*	Ssc.22063.1.S1_at	−0.232	6.94E-04	6.49E-02
		Energy Metabolism			
Cox15 homolog, cytochrome c oxidase assembly protein (yeast)	*COX15*	Ssc.22105.1.S1_at	0.139	6.58E-04	6.38E-02
ATP synthase, H^+ transporting, mitochondrial F1 complex, beta polypeptide	*ATP5B*	Ssc.18170.1.S1_at	−0.289	1.94E-05	1.56E-02
		Folding, Sorting, and Degradation			
Golgi snap receptor complex member 2	*GOSR2*	Ssc.28472.1.S1_at	0.272	4.00E-06	6.04E-03
Syntaxin 18	*STX18*	Ssc.26658.1.A1_at	−0.137	2.18E-04	4.18E-02
		Glycan Biosynthesis and Metabolism			
Dehydrodolichyl diphosphate synthase	*DHDDS*	Ssc.24439.1.A1_at	0.161	5.21E-05	2.37E-02
O-linked N-Acetylglucosamine (Glcnac) transferase (Udp-N-acetylglucosamine:polypeptide-N-acetylglucosaminyl transferase)	*OGT*	Ssc.8000.1.A1_at	−0.140	4.62E-04	5.57E-02
Exostoses (multiple) 1	*EXT1*	Ssc.7562.1.A1_at	−0.167	2.80E-04	4.51E-02
Mannosidase, alpha, class 1A, member 1	*MAN1A1*	Ssc.15489.1.S1_at	−0.324	1.61E-04	3.67E-02
Uronyl-2-sulfotransferase	*UST*	Ssc.29402.1.A1_at	−0.399	9.61E-05	2.86E-02
		Infectious Diseases			
Ero1-like (*S. cerevisiae*)	*ERO1L*	Ssc.2709.1.S1_at	−0.343	1.22E-04	3.10E-02

Continued

Table 3.—*Continued*

KEGG Pathway Theme/Gene Name*	Gene Symbol	Porcine Affy ID	Log2 Fold Change	*P* Value	q-value
		Lipid Metabolism			
Cdp-diacylglycerol–inositol 3-phosphatidyltransferase (phosphatidylinositol synthase)	*CDIPT*	Ssc.21033.2.S1_at	0.243	2.19E-04	4.17E-02
Sterol O-acyltransferase (acyl-coenzyme A: cholesterol acyltransferase) 1	*SOAT1*	Ssc.5643.1.A1_at	−0.208	3.72E-04	5.13E-02
Stearoyl-CoA desaturase 5	*SCD5*	Ssc.14373.1.A1_at	−0.219	8.05E-04	6.98E-02
Glycerol-3-phosphate dehydrogenase 1-like	*GPD1L*	Ssc.24184.1.S1_at	−0.236	1.67E-05	1.44E-02
Phospholipase D1, phosphatidylcholine-specific	*PLD1*	Ssc.7156.1.A1_at	−0.246	2.28E-04	4.20E-02
Elovl family member 5, elongation of long chain fatty acids (Fen1/Elo2, Sur4/Elo3-like, yeast)	*ELOVL5*	Ssc.25062.1.A1_at	−0.270	4.75E-04	5.59E-02
Galactosylceramidase	*GALC*	Ssc.30293.1.A1_at	−0.333	3.96E-06	6.36E-03
		Membrane Transport			
ATP-binding cassette, subfamily C (Cftr/Mrp), member 5	*ABCC5*	Ssc.6425.1.A1_at	−0.252	3.96E-04	5.21E-02
		Metabolism of Other Amino Acids			
Selenophosphate synthetase 1	*SEPHS1*	Ssc.22824.1.S1_at	−0.232	1.67E-04	3.69E-02
		Neurodegenerative Diseases			
Arginine-glutamic acid dipeptide (re) repeats	*RERE*	Ssc.5095.1.A1_at	−0.378	8.58E-07	2.96E-03
		Nucleotide Metabolism			
Uridine-cytidine kinase 2	*UCK2*	Ssc.24728.2.S1_at	0.216	7.82E-04	6.83E-02
Adenylate cyclase 7	*ADCY7*	Ssc.5048.1.S1_at	−0.144	5.32E-04	5.95E-02
Phosphodiesterase 8A	*PDE8A*	Ssc.29579.1.A1_at	−0.208	6.64E-05	2.50E-02
5′-Nucleotidase, ecto (Cd73)	*NT5E*	Ssc.6013.1.A1_at	−0.314	2.34E-06	5.13E-03
Phosphodiesterase 8A	*PDE8A*	Ssc.4651.1.S1_at	−0.352	2.72E-04	4.55E-02
Phosphodiesterase 4D, cAMP-specific (phosphodiesterase e3 dunce homolog, *Drosophila*)	*PDE4D*	Ssc.17233.1.A1_at	−0.522	6.05E-05	2.35E-02
		Sensory System			
Adrenergic, beta, receptor kinase 2	*ADRBK2*	Ssc.9883.1.A1_at	−0.311	3.27E-05	1.92E-02
		Signal Transduction			
Mitogen-activated protein kinase 1	*MAPK1*	Ssc.5106.1.S1_at	0.215	3.50E-04	4.96E-02
Purinergic receptor P2X, ligand-gated ion channel, 4	*P2RX4*	Ssc.18377.1.S1_at	0.137	9.31E-05	2.88E-02
Nuclear factor of activated T cells 5, tonicity-responsive	*NFAT5*	Ssc.17745.1.S1_at	−0.178	1.03E-04	2.95E-02
Calcium channel, voltage-dependent, gamma subunit 8	*CACNG8*	Ssc.18270.1.S1_at	−0.201	3.22E-04	4.79E-02
Neuregulin 3	*NRG3*	Ssc.13323.2.S1_at	−0.203	6.77E-04	6.46E-02
Mitogen-activated protein kinase kinase kinase kinase 4	*MAP4K4*	Ssc.3574.1.A1_at	−0.210	6.19E-04	6.33E-02
Phosphoinositide-3-kinase, regulatory subunit 1 (P85 alpha)	*PIK3R1*	Ssc.10754.1.A1_at	−0.232	2.75E-04	4.52E-02
V-Erb-A erythroblastic leukemia viral oncogene homolog 4 (avian)	*ERBB4*	Ssc.25003.1.S1_at	−0.258	2.08E-04	4.15E-02
Bone morphogenetic protein 5	*BMP5*	Ssc.1179.1.S1_at	0.312	5.80E-05	2.41E-02
Mitogen-activated protein kinase kinase kinase 14	*MAP3K14*	Ssc.13241.1.A1_at	−0.334	1.22E-04	3.08E-02
Fibroblast growth factor receptor 2	*FGFR2*	Ssc.7516.1.A1_at	−0.344	5.21E-04	5.87E-02
Neuregulin 1	*NRG1*	Ssc.4398.1.S1_at	−0.354	9.17E-06	1.16E-02
DNA damage-inducible transcript 4	*DDIT4*	Ssc.4104.1.S1_at	−0.377	1.86E-07	1.49E-03
Latent transforming growth factor beta binding protein 1	*LTBP1*	Ssc.8072.1.A1_at	−0.591	2.49E-05	1.77E-02
		Signaling Molecules and Interaction			
Myelin protein zero-like 1	*MPZL1*	Ssc.30671.1.A1_at	0.290	7.58E-04	6.83E-02
		Ssc.21255.1.S1_at	−0.236	5.44E-04	5.97E-02
Glutamate receptor, ionotropic, kainate 2	*GRIK2*	Ssc.4849.1.A1_at	−0.242	3.78E-04	5.16E-02
		Xenobiotics Biodegradation and Metabolism			
Sirtuin (silent mating type information regulation 2 homolog) 1 (*S. cerevisiae*)	*SIRT1*	Ssc.10786.1.A1_at	−0.283	1.02E-04	3.01E-02
Epoxide hydrolase 1, microsomal (xenobiotic)	*EPHX1*	Ssc.15309.1.S1_at	−0.279	1.16E-04	2.99E-02

*KEGG Pathways were found using DAVID's Functional Annotation tool; Gene names and symbols are the human homologs of porcine genes from the Affymetrix (Affy) array probes (67).

involved in glucose catabolism represented one of the single largest GO enrichment cluster themes that was downregulated and included metabolism and catabolism of very simple and complex carbohydrates (Supplementary Table S10). However, genes involved in cofactor metabolism represented the largest GO enrichment cluster theme and included biosynthesis and metabolism of nucleotides, nucleosides, and ATP (Supplementary Table S10). The fold changes, q, and *P* values of genes involved in MSH-

Table 4. *Liver tissue genes with false discovery rate correction (q-value) cutoff 0.07*

KEGG Pathway Theme/Human Gene Name*	Gene Symbol	Porcine Affy ID	Log2 Fold Change	*P* Value	q-value
		Amino Acid Metabolism			
Methionine adenosyltransferase i, alpha	*MAT1A*	Ssc.27380.1.S1_at	0.391	3.28E-04	5.28E-02
Nuclear receptor binding set domain protein 1	*NSD1*	Ssc.20770.1.S1_at	−0.191	2.43E-04	4.59E-02
Phosphoserine phosphatase	*PSPH*	Ssc.12475.1.A1_at	−0.667	2.16E-04	4.53E-02
		Carbohydrate Metabolism			
Lactate dehydrogenase C	*LDHC*	Ssc.302.1.S1_at	0.251	6.56E-04	6.85E-02
Phospholipase C, gamma 2 (phosphatidylinositol-specific)	*PLCG2*	Ssc.24329.1.A1_at	0.231	9.14E-05	3.20E-02
Transaldolase 1	*TALDO1*	Ssc.1050.1.S1_at	−0.169	4.69E-04	6.12E-02
Malate dehydrogenase 1, Nad (soluble)	*MDH1*	Ssc.11103.1.S1_at	−0.275	2.61E-04	4.77E-02
		Cancers			
Egl nine homolog 1 (*C. elegans*)	*EGLN1*	Ssc.5854.1.S1_at	0.195	1.84E-04	4.59E-02
Baculoviral Iap repeat-containing 5 (survivin)	*BIRC5*	Ssc.432.1.S1_at	−0.383	9.03E-05	3.20E-02
		Cell Communication			
Multiple Pdz domain protein	*MPDZ*	Ssc.23933.1.A1_at	0.491	2.84E-05	1.56E-02
		Ssc.5448.1.S1_at	0.486	2.84E-04	5.04E-02
Tubulin, beta 2A	*TUBB2A*	Ssc.10115.3.S1_a_at	−0.370	2.76E-05	1.55E-02
Tubulin, beta	*TUBB*	Ssc.6903.1.S2_at	−0.385	5.55E-04	6.59E-02
Tubulin, alpha, ubiquitous	*TUBA1C*	Ssc.17154.1.A1_a_at	−0.457	3.03E-04	5.18E-02
Tubulin, beta	*TUBB*	Ssc.6903.1.S1_at	−0.497	6.70E-04	6.79E-02
		Cell Growth and Death			
Retinoblastoma-like 2 (P130)	*RBL2*	Ssc.10727.1.A1_at	0.205	6.05E-04	6.70E-02
Cdc6 cell division cycle 6 homolog (*S. cerevisiae*)	*CDC6*	Ssc.11879.1.A1_at	−0.419	3.83E-05	1.88E-02
		Cell Motility			
Rho guanine nucleotide exchange factor (Gef) 7	*ARHGEF7*	Ssc.17929.1.A1_at	0.249	1.05E-04	3.42E-02
		Energy Metabolism			
Atp Synthase, H^+ transporting, mitochondrial F0 complex, subunit C3 (subunit 9)	*ATP5G3*	Ssc.13371.1.S1_at	−0.166	5.72E-04	6.70E-02
Cytochrome c oxidase subunit VIIC	*COX7C*	Ssc.1461.1.S1_at	−0.335	3.12E-04	5.23E-02
Carbonic anhydrase III, muscle specific	*CA3*	Ssc.10960.1.S1_at	−0.961	3.95E-04	5.64E-02
		Ssc.19866.1.S1_at	−1.061	2.47E-06	4.96E-03
		Folding, Sorting, and Degradation			
Unc-51-like kinase 2 (*C. elegans*)	*ULK2*	Ssc.18729.1.A1_s_at	0.211	7.33E-06	9.30E-03
		Glycan Biosynthesis and Metabolism			
N-deacetylase/N-sulfotransferase (heparan glucosaminyl) 2	*NDST2*	Ssc.6316.1.S1_at	0.163	1.01E-04	3.34E-02
Cdc91 cell division cycle 91-like 1 (*S. cerevisiae*)	*PIGU*	Ssc.22132.1.A1_at	0.151	5.09E-04	6.33E-02
		Immune System			
Toll-like receptor 6	*TLR6*	Ssc.22011.1.S1_at	0.235	3.69E-04	5.57E-02
Complement component 3	*C3*	Ssc.23205.2.A1_at	0.173	2.37E-04	4.66E-02
Coagulation factor IX (plasma thromboplastic component, christmas disease, hemophilia B)	*F9*	Ssc.10446.2.S1_at	0.102	2.99E-04	5.20E-02
		Lipid Metabolism			
Galactosylceramidase	*GALC*	Ssc.7531.1.A1_at	0.486	5.61E-04	6.63E-02
Galactosylceramidase	*GALC*	Ssc.7531.2.S1_at	0.469	3.86E-04	5.62E-02
Ethanolamine kinase 2	*ETNK2*	Ssc.3730.1.S1_at	0.297	6.65E-04	6.80E-02
Phosphatidic acid phosphatase type 2B	*PPAP2B*	Ssc.6233.1.S1_at	0.242	4.48E-04	6.10E-02
Hypothetical gene supported by Ak002212; Ak022822; Bc006985; Nm_018396	*METTL2A*	Ssc.5449.1.S1_at	0.123	4.83E-04	6.23E-02
Phosphatidylserine synthase 2	*PTDSS2*	Ssc.3608.1.S1_at	0.119	5.97E-04	6.67E-02
Sterol O-acyltransferase (acyl-coenzyme A: cholesterol acyltransferase) 1	*SOAT1*	Ssc.19509.1.A1_at	−0.201	4.57E-04	6.13E-02
Putative methyltransferase	*WBSCR22*	Ssc.10992.1.S1_a_at	−0.224	5.30E-04	6.46E-02
Elovl family member 5, elongation of long chain fatty acids (Fen1/Elo2, Sur4/Elo3-like, yeast)	*ELOVL5*	Ssc.1151.1.A1_at	−0.238	2.42E-04	4.60E-02
Platelet-activating factor acetylhydrolase 2, 40 kDa	*PAFAH2*	Ssc.2768.3.S1_at	−0.296	6.96E-04	6.83E-02
Acyl-CoA synthetase long-chain family member 3	*ACSL3*	Ssc.2176.1.A1_at	−0.463	2.29E-04	4.64E-02
Hydroxysteroid (17-beta) dehydrogenase 7	*HSD17B7*	Ssc.12454.1.A1_at	−0.514	2.06E-04	4.60E-02
Fatty acid binding protein 1, liver*	*FABP1*	Ssc.604.1.S1_at	−0.279	2.71E-05	1.56E-02

Continued

Table 4.—*Continued*

KEGG Pathway Theme/Human Gene Name*	Gene Symbol	Porcine Affy ID	Log2 Fold Change	*P* Value	q-value
Fatty acid binding protein 3, muscle and heart (mammary-derived growth inhibitor)*	*FABP3*	Ssc.4360.1.A1_at	−0.614	3.51E-04	5.46E-02
NAD(P)H dehydrogenase, quinone 1	*NQO1*	Ssc.1142.1.S1_at	−0.920	4.87E-04	6.25E-02
Membrane Transport					
ATP-binding cassette, subfamily C (Cftr/Mrp), member 5	*ABCC5*	Ssc.6425.3.A1_at	0.313	1.79E-05	1.35E-02
Metabolism of Cofactors and Vitamins					
Nicotinamide nucleotide adenylyltransferase 3	*NMNAT3*	Ssc.7092.1.A1_at	0.330	2.00E-04	4.65E-02
Aldehyde dehydrogenase 1 family, member A1	*ALDH1A1*	Ssc.6928.1.A1_at	−0.152	5.61E-04	6.60E-02
Aldehyde dehydrogenase 1 family, member A1	*ALDH1A1*	Ssc.24986.1.S1_at	−0.248	5.27E-04	6.46E-02
Nucleotide Metabolism					
Phosphodiesterase 6D, cGMP-specific, rod, delta	*PDE6D*	Ssc.19724.2.S1_at	0.181	1.10E-04	3.49E-02
Nonmetastatic cells 1, protein (Nm23A) expressed in	*NME1*	Ssc.19546.1.S1_at	−0.260	1.14E-06	4.60E-03
Ribonucleotide reductase M2 polypeptide	*RRM2*	Ssc.7111.1.A1_at	−0.808	1.71E-04	4.44E-02
Signaling Molecules and Interaction					
Hypocretin (orexin) receptor 2	*HCRTR2*	Ssc.25690.1.S1_at	0.279	2.57E-05	1.55E-02
Activin A receptor, type IIB	*ACVR2B*	Ssc.24084.1.A1_at	0.193	6.61E-04	6.79E-02
Hyaluronan-mediated motility receptor (Rhamm)	*HMMR*	Ssc.26770.1.S1_at	−0.521	1.04E-05	1.05E-02
Signal Transduction					
Frizzled homolog 1 (*Drosophila*)	*FZD1*	Ssc.3590.1.A1_at	0.308	1.83E-05	1.30E-02
Wingless-type Mmtv integration site family, member 9B	*WNT9B*	Ssc.26099.1.S1_at	0.232	9.01E-06	1.03E-02
Purinergic receptor P2X, ligand-gated ion channel, 4	*P2RX4*	Ssc.18377.1.S1_at	−0.214	4.58E-04	6.11E-02
Purinergic receptor P2X, ligand-gated ion channel, 4	*P2RX4*	Ssc.18377.3.S1_at	−0.215	2.59E-07	1.56E-03
Purinergic receptor P2X, ligand-gated ion channel, 4	*P2RX4*	Ssc.18377.3.S1_a_at	−0.308	2.30E-04	4.61E-02
Stathmin 1/oncoprotein 18	*STMN1*	Ssc.7701.1.A1_at	−0.660	1.89E-04	4.65E-02
Translation					
Ribosomal protein L31	*RPL31*	Ssc.27023.1.S1_at	−0.165	2.41E-04	4.68E-02
Xenobiotics Biodegradation and Metabolism					
Acid phosphatase 5, tartrate resistant	*ACP5*	Ssc.575.1.S1_at	0.374	1.90E-04	4.59E-02

*KEGG Pathways were found using DAVID's Functional Annotation tool; Gene names and symbols are the human homolog of porcine genes from the Affymetrix array probes (67).

nduced changes in carbohydrate and energy metabolism are summarized in Table 5. Other significant GO enrichment cluster themes include carboxylic acid metabolism, sterol biosynthesis, and cellular catabolism, among others (Supplementary Table S10).

The scope of the significantly upregulated transcriptional regulation changes in adipose tissue was considerably less than downregulated transcriptional regulation but also involved major groups of genes associated with both anabolic and catabolic processes (Supplementary Table S11). Genes involved in DNA-dependent transcription were upregulated as were genes involved in regionalization development, regionalization, determination of bilateral symmetry, and cell communication. Additionally, genes that regulate apoptosis and neuron apoptosis in particular were also upregulated in adipose tissue (Table 5 and Supplementary Table S11).

Although the effects of the MC4R genotype in response to MSH identified 290 genes in adipose tissue, GO enrichment cluster analysis only identified one cluster theme nucleocytoplasmic transport with an enrichment score of 1.3 or greater (Supplementary Table S12).

DISCUSSION

Our results demonstrate for the first time in a large domestic animal that central administration of melanocortin receptor agonist NDP-MSH resulted in differentially regulated gene expression in hypothalamus, liver, and adipose tissue. It should be noted that although changes in RNA expression do not always correspond to changes in protein expression or biological response, we suggest that systemic changes in the expression of genes that belong to overrepresented GO or KEGG categories imply a functional change. Although the response in gene expression to NDP-MSH suggests melanocortin system involvement, further work is needed substantiate this hypothesis.

The effect of genotype on the response to NDP-MSH was markedly greater in the number genes differentially regulated for adipose tissue compared with hypothalamus or liver tissue, although feeding response to MC4R agonist was similar across genotypes. We have previously reported that adipose tissue is innervated by adrenergic nerve fibers (34). Moreover, immunocytochemical data revealed that most of the subpopulations of the adrenergic leptin receptor-immunoreactive neurons supplying fat tissue in the pig that were positive for NPY and tyrosine hydroxylase immunoactivity (17) were located in the paraventricular nucleus, ventromedial nucleus, anterior hypothalamic area, preoptic area, arcuate nucleus, and supraoptic nucleus (16). Thus, it is conceivable that these neurons also expressed MC4R and central administration of NDP-MSH may

Table 5. *Fat tissue genes with the top 50-fold change*

KEGG Pathway Theme/Gene Name*	Gene Symbol	Porcine Affy ID	Log2 Fold Change	*P* Value	q-value
		Amino Acid Metabolism			
Rap guanine nucleotide exchange factor (Gef) 4	RAPGEF4	Ssc.22583.1.S1_at	0.721	5.60E-08	1.44E-05
Catechol-O-methyltransferase	COMT	Ssc.785.3.S1_at	−0.703	4.95E-08	1.39E-05
Aldehyde dehydrogenase 4 family, member A1	ALDH4A1	Ssc.5607.1.S1_at	−0.840	4.43E-06	1.92E-04
		Carbohydrate Metabolism			
Phosphoenolpyruvate carboxykinase 1 (soluble)	PCK1	Ssc.22959.1.S1_at	1.394	8.59E-06	2.97E-04
Citrate lyase beta like	CLYBL	Ssc.1137.1.S1_at	0.863	6.63E-04	7.23E-03
Hexokinase 1	HK1	Ssc.5615.1.S1_at	−0.695	2.16E-07	2.93E-05
Aldehyde dehydrogenase 1 family, member B1	ALDH1B1	Ssc.25096.1.A1_at	−0.710	1.68E-04	2.61E-03
Transaldolase 1	TALDO1	Ssc.1050.1.S1_at	−0.716	8.62E-10	2.31E-06
Aconitase 1, soluble	ACO1	Ssc.4767.1.S1_at	−0.763	6.52E-07	5.60E-05
Pyruvate kinase, muscle	PKM2	Ssc.1035.1.S1_at	−0.799	1.49E-06	9.48E-05
Dihydrolipoamide S-acetyltransferase (E2 component of pyruvate dehydrogenase complex)	DLAT	Ssc.14.1.S1_at	−0.922	1.68E-07	2.49E-05
Pyruvate dehydrogenase (lipoamide) beta	PDHB	Ssc.4382.1.S1_at	−1.160	2.03E-08	8.92E-06
Malic enzyme 1, NADP(+)-dependent, cytosolic	ME1	Ssc.16336.1.S1_at	−1.230	6.89E-08	1.53E-05
Hexokinase 2	HK2	Ssc.3509.1.S1_at	−1.579	7.18E-10	2.17E-06
Acyl-CoA synthetase short-chain family member 2	ACAS2	Ssc.27871.1.S1_at	−1.648	7.54E-09	5.87E-06
ATP citrate lyase	ACLY	Ssc.30707.1.S1_at	−1.909	9.43E-08	1.79E-05
		Cell Communication			
Laminin, alpha 2 (merosin, congenital muscular dystrophy)	LAMA2	Ssc.11815.1.A1_s_at	0.710	5.79E-06	2.23E-04
		Cell Motility			
Actin, alpha 2, smooth muscle, aorta	ACTG2	Ssc.10316.1.S1_at	0.680	8.08E-03	4.54E-02
		Cell Growth and Death			
Cytochrome c, somatic	CYCS	Ssc.6694.1.S1_at	−0.672	6.46E-07	5.60E-05
		Energy Metabolism			
Sulfotransferase family, cytosolic, 1A, phenol-preferring, member 3	SULT1A1	Ssc.20006.1.S1_at	1.278	1.76E-06	1.08E-04
Cytochrome c-1	CYC1	Ssc.886.1.S1_at	−0.679	1.23E-08	6.62E-06
NADH dehydrogenase (ubiquinone) Fe-S protein 1, 75 kDa (NADH-coenzyme Q reductase)	NDUFS1	Ssc.10953.1.A1_at	−0.702	5.03E-08	1.38E-05
Ubiquinol-cytochrome c Reductase, Rieske iron-sulfur polypeptide 1	UQCRFS1	Ssc.1854.1.A1_at	−0.709	5.56E-08	1.46E-05
NADH dehydrogenase (ubiquinone) 1 beta subcomplex, 3, 12 kDa	NDUFB3	Ssc.20297.1.S1_at	−0.746	1.06E-08	6.42E-06
ATP synthase, H^+ transporting, mitochondrial F0 complex, subunit C1 (subunit 9)	ATP5G1	Ssc.1649.1.A1_at	−0.789	5.81E-08	1.42E-05
Ubiquinol-cytochrome c reductase, complex III subunit VII, 9.5 kDa	UCRQ_HUMAN	Ssc.17272.1.A1_at	−0.811	8.73E-09	6.58E-06
Carbonic anhydrase III, muscle specific	CA3	Ssc.10960.1.S1_at	−0.842	4.18E-03	2.78E-02
		Glycan Biosynthesis and Metabolism			
Peptidoglycan recognition protein 2	PGLYRP2	Ssc.16628.1.S1_at	−0.745	2.29E-03	1.77E-02
		Lipid Metabolism			
Angiopoietin-like 4†	ANGPTL4	Ssc.8980.1.A1_at	1.413	3.88E-08	1.19E-05
Dehydrogenase/reductase (Sdr family) member 4	DHRS4	Ssc.86.1.S1_at	0.816	7.01E-05	1.39E-03
Carnitine palmitoyltransferase 1A (liver)	CPT1A	Ssc.8974.1.S1_at	0.676	4.44E-09	4.28E-06
24-Dehydrocholesterol reductase	DHCR24	Ssc.19298.2.S1_at	−0.741	7.78E-08	1.66E-05
Hydroxysteroid (17-Beta) dehydrogenase 12	HSD17B12	Ssc.20785.1.A1_at	−0.750	1.05E-08	6.52E-06
Stearoyl-CoA desaturase (delta-9-desaturase)	SCD	Ssc.16159.1.S1_at	−0.758	1.06E-03	1.01E-02
Acetyl-coenzyme A carboxylase alpha	ACACA	Ssc.16018.1.S1_at	−1.017	1.65E-08	7.97E-06
Emopamil binding protein (sterol isomerase)	EBP	Ssc.5045.1.S1_at	−1.026	2.84E-09	3.26E-06
Isopentenyl-diphosphate delta isomerase 1	IDI1	Ssc.6714.1.A1_at	−1.067	3.81E-09	3.99E-06
Fatty acid synthase	FASN	Ssc.25076.2.S1_at	−1.162	2.06E-06	1.18E-04
Lipase, endothelial	LIPG	Ssc.21663.1.A1_at	−1.271	2.51E-07	3.18E-05
		Membrane Transport			
ATP-binding cassette, subfamily A (Abc1), member 1	ABCA1	Ssc.7146.1.A1_at	0.731	5.68E-05	1.19E-03
		Metabolism of Other Amino Acids			
Glutathione peroxidase 3 (plasma)	GPX3	Ssc.19694.1.S1_at	0.724	4.65E-03	3.00E-02

Continued

Table 5.—*Continued*

KEGG Pathway Theme/Gene Name*	Gene Symbol	Porcine Affy ID	Log2 Fold Change	*P* Value	q-value
		Nucleotide Metabolism			
Phosphodiesterase 5A, cGMP-specific	PDE5A	Ssc.30373.1.A1_at	−1.047	4.24E-05	9.57E-04
		Signal Transduction			
Paired box gene 2	PAX2	Ssc.21096.1.S1_at	1.028	3.46E-06	1.62E-04
Mitogen-activated protein kinase 9	MAPK9	Ssc.24337.1.S1_at	0.819	6.76E-06	2.50E-04
Epidermal growth factor (beta-urogastrone)	EGF	Ssc.9392.3.A1_at	−0.812	7.39E-06	2.66E-04
		Signaling Molecules and Interaction			
Major histocompatibility complex, class II, Dr beta 1	HLA-DRB4	Ssc.210.7.S1_x_at	0.888	5.95E-03	3.62E-02
Claudin 5 (transmembrane protein deleted in velocardiofacial syndrome)	CLDN5	Ssc.4227.1.S1_at	0.746	1.33E-07	2.19E-05
Major histocompatibility complex, class I, B	HLA-B	Ssc.18553.1.S1_at	0.743	2.57E-04	3.56E-03
Hyaluronan-mediated motility receptor (rhamm)	HMMR	Ssc.26770.1.S1_at	−0.726	1.52E-04	2.43E-03
Leptin (obesity homolog, mouse)	LEP	Ssc.265.1.S2_at	−0.817	2.29E-06	1.25E-04

†Angiopoietin-like 4 is not in the KEGG pathway theme Lipid Metabolism, but research shows (24a, 75) that angiopoietin-like 4 is highly involved in lipid metabolism in human and swine models. False discovery rate correction (q-value) cutoff 0.07; *KEGG Pathways were found using DAVID's Functional Annotation tool; Gene names and symbols are the human homolog of porcine genes from the Affymetrix array probes (67).

have evoked sympathetic outflow to subcutaneous adipose tissue and the subsequent differential response in gene expression observed in liver and the hypothalamus. To that extent, Song et al. (65) reported that MC4R mRNA that was colocalized in pseudorabies virus-labeled neurons with sympathetic outflow to white adipose tissue was located in hypothalamic paraventricular, suprachiasmatic, arcuate, and dorsomedial nuclei in the male hamster. Furthermore, central administration of melanotan II (MTII), a MC3/4R agonist, resulted in differential activation of sympathetic innervation of white and brown adipose tissue, as measured by norepinephrine turnover and stimulated white adipose tissue lipolysis (7). We suggest that central administration of NDP-MSH evoked sympathetic outflow through activation of the MC4R. However, it should be noted that the colocalization of MC4R with hypothalamic neurons that innervate adipose tissue has not been determined in the pig. Furthermore, because NPD-MSH is an MC3R and MC4R agonist, an effect due to MC3R activation cannot be ruled out.

Energy homeostasis is regulated by close interconnected neuroendocrine and autonomic neural pathways emanating from the hypothalamus as described above (64). Following MC4R stimulation, NPY expression increased, while promelanin-concentrating hormone expression decreased with no change in AGRP and POMC expression. The fact that NPY and MSH have opposing actions in the regulation of appetite and energy balance suggests a possible feedback regulatory mechanism in the regulation of energy balance as previously described by Mounien et al. (55). A notable finding in the present study was that NDP-MSH treatment predominantly downregulated genes involved in two major GO enrichment cluster themes, cell communication and signal transduction. Genes such as SYMP, which encodes for a nuclear protein that functions in the regulation of polyadenylation and promotes gene expression (45), and neuregulin-1 and -3, which interact with EGFR to induce growth and differentiation of epithelial, neuronal, and glial cells (21, 50), were downregulated. Additionally, genes involved in nucleotide metabolism were downregulated; two genes of interest were the phosphodiesterase 4D, cAMP-specific (PDE4D), and PDE8A. These genes play a crucial role as terminators of the cAMP signal and restore cellular responsiveness required for neuroendocrine cells (3).

The effect of feed deprivation on gene expression involves metabolic adaptations to the metabolic state in different tissues and has been previously reported for rodents (28, 41, 62). Several adaptations occur during fasting to maintain energy homeostasis in adipose tissue and liver. In adipose tissue, lipolysis is increased in response to food deprivation and therefore a breakdown of triglycerides, which results in increased free fatty acid (FFA) to be utilized as an energy source by other tissues (25). Moreover, FFA oxidation occurs at the liver, which leads to the production of ketone bodies. In addition, liver glycogen is utilized during the early stages of caloric restriction (15). These events as described above lead to eventual reprogramming of the transcriptional events that follow energy deprivation. We report here that NDP-MSH administration and subsequent activation of the melanocortin system, a key neuronal circuit in energy homeostasis, directly affected peripheral genes that regulated energy, lipid, and carbohydrate metabolism in liver and adipose tissue. The most notable effect in the liver was on genes encoding for enzymes and binding proteins representing lipogenesis, in which nine of the 15 genes were downregulated, such as FABP3, acyl-CoA synthetase long-chain family member 3, and elongation of long chain fatty acids 5. These genes play an essential role in de novo lipid synthesis (57, 66). Moreover, genes involved in energy metabolism, such as CA3, COX7C, and MDH1, were also downregulated. This response to NDP-MSH is indicative of an energy conservation response during fasting and is similar to that reported by Lakhagvadorj et al. (49), in which energy-generating processes such as amino acid metabolism and lipid and steroid biosynthesis in fasted pigs expressing the MC4R D298N variant were also downregulated. Furthermore, recent reports demonstrated that CNS-MC3/4R directly regulates hepatic glucose metabolism (58), thermogenesis in brown adipose tissue (71), and lipolysis in white adipose tissue (7). Moreover, the melanocortin antagonist, SHU9119, stimulated expression of lipogenic genes, sterol regulatory element-binding protein-1C, and PPARγ2, and increased lipid content in the liver (56, 61). In contrast, ICV administration of am MC3/4R

agonist, MTII, reduced hepatic expression of the lipogenic gene, stearoyl-CoA desaturase-1 (SCD1), and pretreatment with SHU9119 reversed this effect (47). Mizuno et al. (54) reported that transgenic POMC expression normalized expression of genes associated with hepatic carbohydrate metabolism such as SCD-1, fatty acid transporter, protein tyrosine phosphatase 1B, and peroxisome proliferator-activated receptor-γ coactivator in leptin-deficient obese mice. The authors suggested that central POMC regulation of the expression of these genes in the liver is most likely via the sympathetic nervous system. Furthermore, Nogueiras et al. (56) reported that inhibition of the MC3/4R promoted lipid uptake, triglyceride synthesis, and fat accumulation, while stimulation of the MC3/4R increased lipid mobilization. These effects were independent of food intake and changes in adiposity.

There are no reports on global transcriptional profiling of adipose tissue after NDP-MSH treatment. In a related study, the expression of several adipose tissue genes was determined after central treatment of a melanocortin agonist in the Siberian hamster (7). These authors were the first to demonstrate that central administration of a melanocortin agonist, MTII, stimulated adipose tissue lipolysis through the sympathetic nervous system in the Siberian hamster (7). However, this study was of limited scope with regard to adipose tissue gene expression data.

A remarkable finding in our study is that NDP-MSH induced upregulated expression of adipose tissue genes involved in the structural morphogenesis and pattern specification of adipose tissue, as indicated by three main GO Biological Processes of development, regionalization, and determination of bilateral symmetry being overrepresented among these genes. Similarly, 3 days of fasting in pigs upregulated expression of adipose tissue genes involved in adipose tissue morphology and structure, since three main GO Biological Processes of cytoskeletal organization, vasculature development, and branching structure development were overrepresented among adipose tissue genes (49). However, NDP-MSH treatment apparently did not influence other angiogenesis-related genes as did 3-day fasting in pigs (49).

Unexpectedly, a group of genes upregulated by NDP-MSH treatment directly or indirectly antagonize lipogenesis or adipogenesis. For instance, ANGPTL4 was strongly upregulated and inhibits LPL activity and angiogenic capacity (11, 26, 31). Interleukin 15 also was upregulated and antagonizes lipogenesis by stimulating hormone-sensitive lipase (2). Furthermore, IGFBP-3 was upregulated and directly or indirectly inhibits adipogenesis (12, 35). Possibly, these genes are collectively involved in dictating the sympathetic catabolic influence on adipose tissue during fasting. Several other unexpected upregulated genes linked to the adipocyte or adipogenesis included pyruvate dehydrogenase kinase, isozyme 4 (PDK4), EGFR, adiponectin, and ANG1. Additionally, UCP3 was also upregulated by NDP-MSH treatment. PDK4 may play a role in sympathetic induced metabolism, since it modulates the activity of adipose tissue glyceroneogenesis (10). Other targets of sympathetic stimulation to adipose tissue included downregulated lipid biosynthetic genes such as FASN, LPL, and leptin.

NDP-MSH induced downregulation of adipose tissue genes involved in energy-generating related processes. Downregulation of genes involved in direct energy-generating processes such as oxidative phosphorylation and TCA was evident after NDP-MSH treatment, and these genes were also prominently downregulated in adipose tissue from fasted rats (46) and pigs fasted for 3 days (49). Our data also demonstrate a metabolic switch toward energy conservation similar to what was observed in pigs fasted for 3 days (49). Downregulation of genes involved in cofactor metabolism in adipose tissue was a major cluster theme for NDP-MSH-treated and fasted pigs (49). Additionally, genes involved in steroid metabolism and biosynthesis were downregulated in NDP-MSH-treated and fasted pigs (49). An exception to these downregulated steroid metabolism and biosynthesis genes was a marked upregulation of HSD3B1 in NDP-MSH-treated pigs. The HSD3B1 enzymatic system plays a role in the biosynthesis of all classes of hormonal steroids (72). The significance of upregulated HSD3B1 in NDP-MSH-treated pigs remains to be determined. Similarity of many gene cluster themes of downregulated genes indicates that changes in gene expression was similar for NDP-MSH-treated pigs and those fasted for 3 days (49). Our studies indicate that much of the fasting response may be attributable to stimulation of MC4R altering sympathetic flow into adipose tissue.

Conclusions

The results of the present study demonstrate that the transcriptional response to central administration of NDP-MSH in part was similar to a metabolic response to energy deprivation as previously reported in the pig (49). At the transcriptional level, genes involved in lipid and carbohydrate metabolism in liver and adipose tissue were differentially regulated following NDP-MSH treatment depending on their anabolic/catabolic function. In particular, a decrease in the expression of hepatic and adipose tissue lipogenic genes occurred within 24 h posttreatment. Furthermore, a unique group of genes that can directly or indirectly antagonize lipogenesis or adipogenesis were upregulated by NDP-MSH treatment in adipose tissue. Most notably, ANGPTL4 was strongly upregulated and inhibits LPL activity and angiogenic capacity. Possibly, these genes dictate the sympathetic catabolic influence on adipose tissue during fasting. Although the results have put forward novel ideas, further work is needed to substantiate the adaptive response in gene expression to NDP-MSH.

ACKNOWLEDGMENTS

The authors thank Brent Jackson, Lara Lee-Rutherford, John Gamble, and Carl Rogers.

Mention of a trade name, proprietary product, or specific equipment does not constitute a guarantee or warranty by the U.S. Department of Agriculture, the University of Georgia or Iowa State University and does not imply its approval to the exclusion of other products that may be suitable.

GRANTS

This research was supported by United States Department of Agriculture, National Research Initiative Grant USDA-NRI-2005-3560415618 and state and hatch funds allocated to the Georgia Agriculture Experiment Station.

DISCLOSURES

No conflicts of interest, financial or otherwise, are declared by the authors.

REFERENCES

1. **Adan RA, Tiesjema B, Hillebrand JJ, la Fleur SE, Kas MJ, de Krom M.** The MC4 receptor and control of appetite. *Br J Pharmacol* 149: 815–827, 2006.

2. **Ajuwon KM, Spurlock ME.** Direct regulation of lipolysis by interleukin-15 in primary pig adipocytes. *Am J Physiol Regul Integr Comp Physiol* 287: R608–R611, 2004.
3. **Ang KL, Antoni FA.** Reciprocal regulation of calcium dependent and calcium independent cyclic AMP hydrolysis by protein phosphorylation. *J Neurochem* 81: 422–433, 2002.
4. **Barb CR, Chang WC, Leshin LS, Rampacek GB, Kraeling RR.** Opioid modulation of gonadotropin releasing hormone release from the hypothalamic preoptic area in the pig. *Domest Anim Endocrinol* 11: 375–382, 1994.
5. **Barb CR, Kraeling RR, Estienne MJ, Rampacek GB.** Technique for cannulation of the lateral ventricle of the brain in swine. *Kopf Carrier* 35: 1–5, 1993.
6. **Barb CR, Robertson AS, Barrett JB, Kraeling RR, Houseknecht KL.** The role of melanocortin-3 and -4 receptor in regulating appetite, energy homeostasis and neuroendocrine function in the pig. *J Endocrinol* 181: 39–52, 2004.
7. **Brito MN, Brito NA, Baro DJ, Song CK, Bartness TJ.** Differential activation of the sympathetic innervation of adipose tissues by melanocortin receptor stimulation. *Endocrinology* 148: 5339–5347, 2007.
8. **Butler AA.** The melanocortin system and energy balance. *Peptides* 27: 281–290, 2006.
9. **Butler AA, Cone RD.** Knockout models resulting in the development of obesity. *Trends Genet* 17: S50–S54, 2001.
10. **Cadoudal T, Distel E, Durant S, Fouque F, Blouin JM, Collinet M, Bortoli S, Forest C, Benelli C.** Pyruvate dehydrogenase kinase 4: regulation by thiazolidinediones and implication in glyceroneogenesis in adipose tissue. *Diabetes* 57: 2272–2279, 2008.
11. **Cazes A, Galaup A, Chomel C, Bignon M, Brechot N, Le Jan S, Weber H, Corvol P, Muller L, Germain S, Monnot C.** Extracellular matrix-bound angiopoietin-like 4 inhibits endothelial cell adhesion, migration, and sprouting and alters actin cytoskeleton. *Circ Res* 99: 1207–1215, 2006.
12. **Chan SS, Schedlich LJ, Twigg SM, Baxter RC.** Inhibition of adipocyte differentiation by insulin-like growth factor-binding protein-3. *Am J Physiol Endocrinol Metab* 296: E654–E663, 2009.
13. **Chu TM, Weir B, Wolfinger R.** A systematic statistical linear modeling approach to oligonucleotide array experiments. *Math Biosci* 176: 35–51, 2002.
14. **Cone RD.** The central melanocortin system and its role in energy homeostasis. *Ann Endocrinol (Paris)* 60: 3–9, 1999.
15. **Corssmit EP, Romijn JA, Sauerwein HP.** Regulation of glucose production with special attention to nonclassical regulatory mechanisms: a review. *Metabolism* 50: 742–755, 2001.
16. **Czaja K, Kraeling RR, Barb CR.** Are hypothalamic neurons transsynaptically connected to porcine adipose tissue? *Biochem Biophys Res Commun* 311: 482–485, 2003.
17. **Czaja K, Lakomy M, Sienkiewicz W, Kaleczyc J, Pidsudko Z, Barb CR, Rampacek GB, Kraeling RR.** Distribution of neurons containing leptin receptors in the hypothalamus of the pig. *Biochem Biophys Res Commun* 298: 333–337, 2002.
18. **Dennis G, Jr, Sherman BT, Hosack DA, Yang H, Gao W, Lance HC, Lempicki RA.** DAVID: Database for Annotation, Visualization, and Integrated Discovery. *Genome Biol* 4: P3, 2003.
19. **Dyer CJ, Touchette KJ, Allee GL, Carroll JA, Matteri RL.** Porcine melanocortin agouti-related peptide: cloning, tissue distribution and quantification of size-related differences in gene expression. *J Anim Sci* 78: 45, 2000.
20. **Estienne MJ, Kesner JS, Barb CR, Kraeling RR, Rampacek GB, Estienne CE.** Gonadotropin and prolactin secretion following intraventricular administration of morphine in gilts. *Exp Biol Med (Maywood)* 193: 92–97, 1990.
21. **Falls DL.** Neuregulins: functions, forms, and signaling strategies. *Exp Cell Res* 284: 14–30, 2003.
22. **Fan ZC, Sartin JL, Tao YX.** Molecular cloning and pharmacological characterization of porcine melanocortin-3 receptor. *J Endocrinol* 196: 139–148, 2008.
23. **Fan ZC, Sartin JL, Tao YX.** Pharmacological analyses of two naturally occurring porcine melanocortin-4 receptor mutations in domestic pigs. *Domest Anim Endocrinol* 34: 383–390, 2008.
24. **Farooqi IS, Yeo GS, Keogh JM, Aminian S, Jebb SA, Butler G, Cheetham T, O'Rahilly S.** Dominant and recessive inheritance of morbid obesity associated with melanocortin 4 receptor deficiency. *J Clin Invest* 106: 271–279, 2000.

24a. **Feng SQ, Chen XD, Xia T, Gan L, Qiu H, Dai MH, Zhou L, Peng Y, Yang ZQ.** Cloning, chromosome mapping and expression characteristics of porcine ANGPTL3 and -4. *Cytogenet Genome Res* 114:44–49, 2006.

25. **Finn PF, Dice JF.** Proteolytic and lipolytic responses to starvation. *Nutrition* 22: 830–844, 2006.
26. **Galaup A, Cazes A, Le Jan S, Philippe J, Connault E, Le Coz E, Mekid H, Mir LM, Opolon P, Corvol P, Monnot C, Germain S.** Angiopoietin-like 4 prevents metastasis through inhibition of vascular permeability and tumor cell motility and invasiveness. *Proc Natl Acad Sci USA* 103: 18721–18726, 2006.
27. **Giraudo SQ, Billington CJ, Levine AS.** Feeding effects of hypothalamic injection of melanocortin 4 receptor ligands. *Brain Res* 809: 302–306, 1998.
28. **Gosmain Y, Dif N, Berbe V, Loizon E, Rieusset J, Vidal H, Lefai E.** Regulation of SREBP-1 expression and transcriptional action on HKII and FAS genes during fasting and refeeding in rat tissues. *J Lipid Res* 46: 697–705, 2005.
29. **Graham M, Shutter JR, Sarmiento U, Sarosi I, Stark KL.** Overexpression of Agrt leads to obesity in transgenic mice. *Nature Genet* 17: 273–274, 1997.
30. **Hart HA, Azain MJ, Hausman GJ, Reeves DE, Barb CR.** Failure of short term feed restriction to affect luteinizing hormone and leptin secretion or subcutaneous adipose tissue expression of leptin in the prepuberal gilt. *Can J Anim Sci* 87: 191–197. 2007.
31. **Hato T, Tabata M, Oike Y.** The role of angiopoietin-like proteins in angiogenesis and metabolism. *Trends Cardiovasc Med* 18: 6–14, 2008.
32. **Hausman GJ, Barb CR, Dean RG.** Patterns of gene expression in pig adipose tissue: transforming growth factors, interferons, interleukins and other cytokines. *J Anim Sci* 85: 2445–2456, 2007.
33. **Hausman GJ, Barb CR, Dean RG.** Patterns of gene expression in pig adipose tissue: Insulin-like growth factor system proteins, neuropeptide Y (NPY), NPY receptors, neurotrophic factors and other secreted factors. *Domest Anim Endocrinol* 35: 24–34, 2008.
34. **Hausman GJ, Richardson RL.** Adrenergic innervation of fetal pig adipose tissue. *Histochem Ultrastruct Stud Acta Anat (Basel)* 130: 291–297, 1987.
35. **Hausman GJ, Richardson RL, Simmen FA.** Secretion of insulin-like growth factor (IGF)-I and -II and IGF binding proteins (IGFBPs) in fetal stromal-vascular (S-V) cell cultures obtained before and after the onset of adipogenesis in vivo. *Growth Dev Aging* 66: 11–26, 2002.
36. **Hochberg Z, Benjamini Y.** Controlling the false discovery rate: a practical and powerful approach to multiple testing. *J Royal Stat Soc* B: 289–300, 1995.
37. **Irizarry RA, Bolstad BM, Collin F, Cope LM, Hobbs B, Speed.** Summaries of Affymetrix GeneChip probe level data. *Nucl Acids Res* 31: e15, 2003.
38. **Kanehisa M, Araki M, Goto S, Hattori M, Hirakawa M, Itoh M, Katayama T, Kawashima S, Okuda S, Tokimatsu T, Yamanishi Y.** KEGG for linking genomes to life and the environment. *Nucl Acids Res* 36: D480–D484, 2008.
39. **Kanehisa M, Goto S.** KEGG: Kyoto encyclopedia of genes and genomes. *Nucl Acids Res* 28: 27–30, 2000.
40. **Kanehisa M, Goto S, Hattori M, Aoki-Kinoshita KF, Itoh M, Kawashima S, Katayama T, Araki M, Hirakawa M.** From genomics to chemical genomics: new developments in KEGG. *Nucl Acids Res* 34: D354-D357, 2006.
41. **Kersten S, Seydoux J, Peters JM, Gonzalez FJ, Desvergne B, Wahli W.** Peroxisome proliferator-activated receptor alpha mediates the adaptive response to fasting. *J Clin Invest* 103: 1489–1498, 1999.
42. **Kim KS, Larsen N, Short T, Plastow G, Rothschild MF.** A missense variant of the porcine melanocortin-4 receptor (MC4R) gene is associated with fatness, growth, and feed intake traits. *Mamm Genome* 11: 131–135, 2000.
43. **Kim KS, Reecy JM, Hsu WH, Anderson LL, Rothschild MF.** Functional and phylogenetic analyses of a melanocortin-4 receptor mutation in domestic pigs. *Domest Anim Endocrinol* 26: 75–86, 2004.
44. **Kineman RD, Kraeling RR, Crim JW, Leshin LS, Barb CR, Rampacek GB.** Localization of proopiomelanocortin (POMC) immunoreactive neurons in the forebrain of the pig. *Biol Reprod* 40: 1119–1126, 1989.
45. **Kolev NG, Steitz JA.** Symplekin and multiple other polyadenylation factors participate in 3′-end maturation of histone mRNAs. *Genes Dev* 19: 2583–2592, 2005.
46. **Li RY, Zhang QH, Liu Z, Qiao J, Zhao SX, Shao L, Xiao HS, Chen JL, Chen MD, Song HD.** Effect of short-term and long-term fasting on

transcriptional regulation of metabolic genes in rat tissues. *Biochem Biophys Res Commun* 344: 562–570, 2006.
47. **Lin J, Choi YH, Hartzell DL, Li C, Della-Fera MA, Baile CA.** CNS melanocortin and leptin effects on stearoyl-CoA desaturase-1 and resistin expression. *Biochem Biophys Res Commun* 311: 324–328, 2003.
48. **Littell RC, Milliken GA, Stroup WW, Wolfinger RD.** SAS (R) System for mixed models. *SAS Inst Inc, Cary, NC* 1996.
49. **Lkhagvadorj S, QL, Cai W, Couture OP, Barb CR, Hausman GJ, Nettleton D, Anderson LL, Dekkers JCM, Tuggle CK.** Microarray gene expression profiles of fasting induced changes in liver and adipose tissues of pigs expressing the melanocortin-4 receptor D298N variant. *Physiol Genomics* 38: 98–111, 2009.
50. **Lok J, Sardi SP, Guo S, Besancon E, Ha DM, Rosell A, Kim WJ, Corfas G, Lo EH.** Neuregulin-1 signaling in brain endothelial cells. *J Cereb Blood Flow Metab* 29: 39–43, 2009.
51. **Lubrano-Berthelier C, Cavazos M, Le Stunff C, Haas K, Shapiro A, Zhang S, Bougneres P, Vaisse C.** The human MC4R promoter: characterization and role in obesity. *Diabetes* 52: 2996–3000, 2003.
52. **Marsh DJ, Hollopeter G, Huszar D, Laufer R, Yagaloff KA, Fisher SL, Burn P, Palmiter RD.** Response of melanocortin-4 receptor-deficient mice to anorectic and orexigenic peptides. *Nat Genet* 21: 119–122, 1999.
53. **Meehan TP, Tabeta K, Du X, Woodward LS, Firozi K, Beutler B, Justice MJ.** Point mutations in the melanocortin-4 receptor cause variable obesity in mice. *Mamm Genome* 17: 1162–1171, 2006.
54. **Mizuno TM, Kelley KA, Pasinetti GM, Roberts JL, Mobbs CV.** Transgenic neuronal expression of proopiomelanocortin attenuates hyperphagic response to fasting and reverses metabolic impairments in leptin-deficient obese mice. *Diabetes* 52: 2675–2683, 2003.
55. **Mounien L, Bizet P, Boutelet I, Vaudry H, Jegou S.** Expression of melanocortin MC3 and MC4 receptor mRNAs by neuropeptide Y neurons in the rat arcuate nucleus. *Neuroendocrinology* 82: 164–170, 2005.
56. **Nogueiras R, Wiedmer P, Perez-Tilve D, Veyrat-Durebex C, Keogh JM, Sutton GM, Pfluger PT, Castaneda TR, Neschen S, Hofmann SM, Howles PN, Morgan DA, Benoit SC, Szanto I, Schrott B, Schurmann A, Joost HG, Hammond C, Hui DY, Woods SC, Rahmouni K, Butler AA, Farooqi IS, O'Rahilly S, Rohner-Jeanrenaud F, Tschop MH.** The central melanocortin system directly controls peripheral lipid metabolism. *J Clin Invest* 117: 3475–3488, 2007.
57. **NRC.** *Nutrient Requirements of Pigs*. Washington, DC: National Academy, 1998.
58. **Obici S, Feng Z, Tan J, Liu L, Karkanias G, Rossetti L.** Central melanocortin receptors regulate insulin action. *J Clin Invest* 108: 1079–1085, 2001.
59. **Oosterom J, Garner KM, den Dekker WK, Nijenhuis WA, Gispen WH, Burbach JP, Barsh GS, Adan RA.** Common requirements for melanocortin-4 receptor selectivity of structurally unrelated melanocortin agonist and endogenous antagonist, Agouti protein. *J Biol Chem* 276: 931–936, 2001.
60. **Pfaffl MW, Horgan G, Dempfle L.** Relative expression software tool (REST©) for group-wise comparison and statistical analysis of relative expression results in real-time PCR. *Nucl Acids Res* 30: e36, 2002.
61. **Poritsanos NJ, Wong D, Vrontakis ME, Mizuno TM.** Regulation of hepatic PPARgamma2 and lipogenic gene expression by melanocortin. *Biochem Biophys Res Commun* 376: 384–388, 2008.
62. **Ryu MH, Daily JW 3rd, Cha YS.** Effect of starvation on hepatic acyl-CoA synthetase, carnitine palmitoyltransferase-I, and acetyl-CoA carboxylase mRNA levels in rats. *Nutrition* 21: 537–542, 2005.
63. **SAS.** *SAS User's Guide (release 8.0)*. Cary, NC: Statistical Analysis Systems Institute, 1999.
64. **Seeley RJ, Drazen DL, Clegg DJ.** The critical role of the melanocortin system in the control of energy balance. *Annu Rev Nutr* 24: 133–149, 2004.
65. **Song CK, Jackson RM, Harris RB, Richard D, Bartness TJ.** Melanocortin-4 receptor mRNA is expressed in sympathetic nervous system outflow neurons to white adipose tissue. *Am J Physiol Regul Integr Comp Physiol* 289: R1467–R1476, 2005.
66. **Soupene E, Kuypers FA.** Mammalian long-chain acyl-CoA synthetases. *Exp Biol Med (Maywood)* 233: 507–521, 2008.
67. **Tasi S, Cassady JP, Freking BA, Nonneman DJ, Rohrer GA, Piedrahita JA.** Annotation of the Affymetrix porcine genome microarray. *Anim Genet* 37: 423–424, 2006.
68. **Tatro JB.** Receptor biology of the melanocortins, a family of neuroimmunomodulatory peptides. *Neuroimmunomodulation* 3: 259–284, 1996.
69. **Vaisse C, Clement K, Durand E, Hercberg S, Guy-Grand B, Froguel P.** Melanocortin-4 receptor mutations are a frequent and heterogeneous cause of morbid obesity. *J Clin Invest* 106: 253–262, 2000.
70. **Vergoni AV, Schioth HB, Bertolini A.** Melanocortins and feeding behavior. *Biomed Pharmacother* 54: 129–134, 2000.
71. **Voss-andreae A, Murphy JG, Ellacott KL, Stuart RC, Nillni EA, Cone RD, Fan W.** Role of the central melanocortin circuitry in adaptive thermogenesis of brown adipose tissue. *Endocrinology* 148: 1550–1560, 2007.
72. **Wang L, Salavaggione E, Pelleymounter L, Eckloff B, Wieben E, Weinshilboun R.** Human 3β-hydroxysteroid dehydrogenase types 1 and 2: Gene sequence variation and functional genomics. *J Steroid Biochem Mol Biol* 107: 88–99, 2007.
73. **Wirth MM, Giraudo SQ.** Agouti-related protein in the hypothalamic paraventricular nucleus: effect on feeding. *Peptides* 21: 1369–1375, 2000.
74. **Wolfinger RD, Gibson G, Wolfinger ED, Bennett L, Hamadeh H, Bushel P, Afshari C, Paules RS.** Assessing gene significance from cDNA microarray expression data via mixed models. *J Comput Biol* 8: 625–637, 2001.
75. **Yoshida K, Shimizugawa T, Ono M, Furukawa H.** Angiopoietin-like protein 4 is a potent hyperlipidemia-inducing factor in mice and inhibitor of lipoprotein lipase. *J Lipid Res* 43: 1770–1772, 2002.